

# Ground-State Photoelectron Circular Dichroism of Methyl *p*-Tolyl Sulfoxide by Single-Photon Ionisation from a Table-Top Source

Max D. J. Waters,<sup>[a]</sup> Nicolas Ladda,<sup>[b]</sup> Arne Senftleben,<sup>[b]</sup> Vít Svoboda<sup>+</sup>,<sup>[a]</sup>  
Mikhail Belozertsev,<sup>[a, c]</sup> Thomas Baumert,<sup>[b]</sup> and Hans Jakob Wörner<sup>\*[a]</sup>

Single-photon ionisation of enantiopure methyl *p*-tolyl sulfoxide by circularly polarised light at 133 nm shows remarkably strong photoelectron circular dichroism (PECD), which has been measured in a velocity-map-imaging spectrometer. Both enantiomers were measured, each showing a PECD of a similar magnitude (ca. 25%). These experiments were carried out with a tabletop high-harmonic source with a photon energy of 9.3 eV, capable of ionising the electronic ground state of most organic and inorganic molecules. *Ab-initio* scattering calcula-

tions provide a theoretical value of the expected chiral asymmetry parameter, and agree very well with the measured values once orbital mixing via configuration interaction in the cation is taken into account. This study demonstrates a simple photoionisation scheme that can be readily applied to study the time-resolved PECD of photochemical reactions and suggests a pronounced sensitivity of PECD to electronic configuration interaction in the cation.

## Introduction

Molecular chirality is a rich field of study, with many interesting and important applications. Most famously (or rather, infamously), it is of particular importance in pharmaceutical sciences, where including the opposite enantiomer of a medicinal molecule in a drug can have grim consequences.<sup>[1]</sup> Therefore, proper determination of both the handedness and the enantiopurity of an ensemble of chiral molecules holds a lot of interest. However, chirality from a more principal, and basic science perspective, has garnered research since the 19th century, notably in the work of Pasteur.<sup>[2]</sup> These early ideas and studies have been developed further over the centuries, to the point where we now see the fundamental importance of molecular chirality to biology, a fact which is manifested in the homochirality of life.<sup>[3]</sup>

Given this interest, it is no surprise that there have been many and varied efforts to develop experiments that are sensitive to molecular chirality in an interaction-free gas-phase environment.<sup>[4–9]</sup> One such promising avenue is in measuring the forward/backward asymmetry in the photoemission angle of a chiral sample that has been ionised with circularly polarised light, known as photoelectron circular dichroism (PECD). This effect was first predicted in 1976, but was not observed until 2000.<sup>[10,11]</sup> PECD is much stronger than absorptive circular dichroism due to the fact that the chiral response arises in the electric-dipole approximation.<sup>[12]</sup> Since this first measurement, this technique has been the focus of a wide variety of experimental and theoretical studies,<sup>[13–19]</sup> as it is a highly sensitive probe of photoionisation dynamics and molecular structure.<sup>[16]</sup>

In brief, the PECD arises due to the outgoing electrons scattering with the effective molecular potential, causing an asymmetry in the forward-backward distribution of the photoelectrons with respect to the incoming circular light.<sup>[16,20]</sup> This asymmetry can be observed with randomly oriented chiral molecules, but an enhancement for some orientations and decrease for others has been reported.<sup>[21,22]</sup> The scattering is highly sensitive to both the orbital from which the electron originates and the molecular potential, even at quite extended ranges (in comparison to the spatial extent of the molecule), making it difficult to construct intuition that relates the magnitude of PECD to chemical structure or the orbital which is being ionised.<sup>[20,23,24]</sup>

In this work, single-photon PECD is observed from the electronic ground state of a molecule in a velocity-map-imaging (VMI) spectrometer using a tabletop source. In contrast to earlier work based on elliptically polarised sources,<sup>[25]</sup> we use a different high-harmonic-generation source capable of producing quasi-circularly polarised vacuum-ultraviolet (VUV)

[a] M. D. J. Waters, Dr. V. Svoboda,<sup>+</sup> M. Belozertsev, Prof. Dr. H. J. Wörner  
Laboratory of Physical Chemistry, ETH Zürich  
Vladimir-Prelog-Weg 2, 8093 Zürich, Switzerland  
E-mail: hwoerner@ethz.ch  
Homepage: <https://atto.ethz.ch/>

[b] N. Ladda, Dr. A. Senftleben, Prof. Dr. T. Baumert  
Universität Kassel  
Heinrich-Plett-Str. 40, 34132 Kassel, Germany

[c] M. Belozertsev  
Department Chemie, Ludwig-Maximilians-Universität München  
81377 München, Germany

[<sup>+</sup>] Current address: JILA, University of Colorado, Boulder, and the National Institute of Standards and Technology, Boulder, Colorado 80309, U. S.

© 2022 The Authors. ChemPhysChem published by Wiley-VCH GmbH. This is an open access article under the terms of the Creative Commons Attribution Non-Commercial NoDerivs License, which permits use and distribution in any medium, provided the original work is properly cited, the use is non-commercial and no modifications or adaptations are made.

radiation.<sup>[26]</sup> One of the key advantages of the methodology presented in this text is the use of a single-photon ionisation source. Indeed, the strength of high-harmonic sources in laser spectroscopy has been demonstrated before – even within the context of molecular chirality.<sup>[25,27–32]</sup> However, our work sets itself apart by using a single, low-order harmonic (133 nm, H3 of 400 nm) in the ionisation process.<sup>[27]</sup> A key strength of these sources for measuring PECD is that they provide access to coherent, circularly-polarised photons with sufficient energy to ionise electronic ground states, while being significantly cheaper, and more space-efficient, than a synchrotron. In the past, tabletop experiments have measured PECD through multiphoton and strong-field ionisation.<sup>[18,19,33,34]</sup> These techniques are very powerful tools, and provide a great deal of information. However, the photoelectron spectrum produced by single-photon ionisation is much simpler to interpret, and has the benefit of directly accessing the electronic ground state, making the extension to time-resolved experiments far more straightforward. In addition to the simplification of the photoelectron spectrum, the form of the photoelectron angular distribution is also simplified. In our measurements, the only asymmetry term which plays a role in the photoelectron angular distribution is the first-order asymmetry term  $b_1$ , which is in strong contrast to multiphoton measurements where much higher-order Legendre polynomial terms need to be included to fully describe the PECD.<sup>[13]</sup>

The molecule used for the present experiments is methyl *p*-tolyl sulfoxide (MTSO). The structure of MTSO is shown in the schematic diagram shown in Figure 1. The chiral centre is the sulfur atom, which is a tetrahedral centre and has a calculated (optimised at the B3LYP/6-311++G\*\* level-of-theory) methyl-out-of-plane angle (defined as the degree by which the methyl group deviates from the plane passing through the sulfur atom, oxygen atom, and the tolyl group) of 109.4°. The sphere expanding from the molecule in Figure 1 represents the photoionisation Newton sphere, with the different colours representing the differences in photoemission in the forwards and backwards hemispheres, with respect to the incoming light.

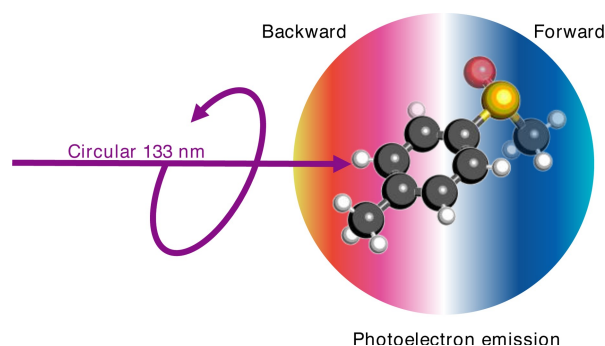


**Figure 1.** Schematic of the experimental principle, where gas-phase methyl *p*-tolyl sulfoxide is ionised with a single photon of circularly polarised light with a wavelength of 133 nm. The sulfur is a chiral centre in this molecule, which leads to a difference in the forwards and backwards emission of photoelectrons, which we observe in a velocity map imaging spectrometer.

From a chemical perspective, MTSO is quite an interesting example of molecular chirality, due to the fact that the chiral centre is bonded to only three different substituents with the fourth “substituent” being a lone electron pair on the sulfur atom. Previous PECD measurements have been focussed on carbon chiral centres, a notable exception being recent work studying a ruthenium complex.<sup>[35]</sup> Additionally, chiral sulfoxides are known to be of particular use in the asymmetric synthesis of pharmaceutically important molecules.<sup>[36,37]</sup> While this use makes sulfoxides an important class of compounds as both starting reagents and final products, it can be highly challenging to determine accurate values for the enantiomeric excess of sulfoxides via high-performance liquid chromatography (HPLC) due to the tendency of the enantiomers to self-disproportionate.<sup>[38,39]</sup> For this reason, it is desirable to have a robust methodology to determine enantiomeric excess, which can deal with interaction-free molecules as this would prevent the self-disproportionation of enantiomers. To this end, gas-phase VMI by single-photon ionisation of the electronic ground state with a circularly polarised source represents just such a robust method.

## Methods

### Experimental

The spectrometer used in this study is a velocity-map-imaging (VMI) spectrometer that has been described in detail with the beamline elsewhere.<sup>[27]</sup> In brief, 800 nm laser light is produced by a Coherent Legend Elite Duo regeneratively amplified laser system, and compressed to a pulse duration of ca. 30 fs. This is frequency doubled in a  $\beta$ -barium borate crystal to obtain 400 nm, which is circularly polarised with a quarter-wave plate and subsequently used to generate quasi-circularly polarised low-order harmonics in a gas cell filled with 10 mbar of xenon as the generation gas.<sup>[26]</sup> This favours the output of the third harmonic (H3, 133 nm), which is further selected using dielectric mirrors (Layertec). The polarisation state of this source has been completely characterised using reflective in-vacuum polarimetry and benchmark PECD measurements, showing that the magnitude of the third Stokes parameter of this source amounted to  $S_3 = 0.96 \pm 0.02$ .<sup>[26]</sup>

*R*-(+)-MTSO (Sigma–Aldrich, 99% enantiomeric excess (HPLC), 99% purity) and *S*-(-)-MTSO (Sigma–Aldrich, 99% enantiomeric excess (HPLC), 99% purity) were used without further purification. MTSO was delivered into the interaction region by supersonic expansion of gas-phase MTSO in a molecular beam using helium as a carrier gas, which then passes through a 1 mm nickel skimmer. The nozzle for this experiment was a high-temperature, high-repetition-rate Even-Lavie valve. MTSO was heated to 87 °C, and the backing pressure of helium is 0.5 bar.

### Computational

For the calculations of the PECD, the geometry of MTSO was optimised at the RHF/cc-pVDZ level of theory using the ORCA 4.2.1 program package.<sup>[47]</sup> The wavefunction which would be used for the subsequent scattering calculations was then calculated using G09 at the RHF/cc-pVTZ level of theory.<sup>[52]</sup> There is no post Hartree–Fock (HF) treatment as ePolyScat requires HF-type wavefunctions. This does not pose an issue in this case, as the electronic ground

state of the neutral molecule can be sufficiently well described with a HF-type wavefunction. The photoelectron kinetic energy-dependent scattering calculations are carried out using ePolyScat.<sup>[44,45]</sup> Using a methodology developed in-house, the chiral coefficient  $b_1$  is extracted from the photoionization matrix elements. This methodology expresses the photoionisation cross-section in terms of the photoionisation matrix elements as a partial-wave expansion in spherical harmonics. This new methodology provides a robust alternative to other methods found in the literature, for example CMS- $X\alpha$  or B-spline.<sup>[42,53, 54]</sup>

## Results and Discussion

Measuring the PECD in VMI requires one to measure two photoelectron images, one in which the sample has been ionised with left-circularly polarised (LCP) light and one with right-circularly polarised (RCP) light. The PECD image can then be obtained by taking the normalised difference of the normalised LCP image ( $I_{LCP}(r, \theta)$ ) and the normalised RCP image ( $I_{RCP}(r, \theta)$ ):

$$PECD(r, \theta) = \frac{2 \cdot (I_{LCP}(r, \theta) - I_{RCP}(r, \theta))}{(I_{LCP}(r, \theta) + I_{RCP}(r, \theta))} \quad (1)$$

where  $r$  is the radius of the photoelectron image from the centre, and is proportional to the square root of the photoelectron kinetic energy, and  $\theta$  is the polar angle and corresponds to the angle of photoelectron emission, with respect to the propagation direction of the incoming light. To obtain the chiral asymmetry parameter  $b_1$ , we first inverted the measured LCP and RCP images using the rBasex algorithm, as implemented in PyAbel and used these to obtain the PECD image, following Eq. (1).<sup>[40]</sup> The resulting image was then antisymmetrised, and the mean was taken within a radial range that corresponded to the photoelectron kinetic energies of interest for each angle ( $I_{PECD}(\theta)$ ). We have then fitted the angular distribution to Eq. (2):

$$I_{PECD}(\theta) = 2b_1^{(+1)} \cos\theta \quad (2)$$

The full details of this analysis method are outlined in detail within several sources from the available literature.<sup>[14,41]</sup>

To verify the circularity of the 133 nm ionising radiation that was used for this study, the PECD of fenchone was measured, where benchmark data from a synchrotron source at the same wavelength is available.<sup>[42]</sup> The measured  $2b_1$  parameter for electronic ground state HOMO photoionisation of *S*-(+)-fenchone from our measurements is compared to 0.154 of the benchmark.<sup>[42]</sup> As the magnitude of PECD is directly related to the magnitude of the Stokes parameter  $S_3$ , we extracted a value of  $|S_3| = 0.96 \pm 0.02$ , which is consistent with our previous results.<sup>[26]</sup>

The static photoelectron spectrum of MTSO is shown in Figure 2. The vertical ionisation potential of MTSO has been reported to be 8.70 eV.<sup>[43]</sup> Given that we ionised with 133 nm light (9.3 eV), we expect photoelectrons with a kinetic energy of ca. 0.6 eV. In our spectrum, the peak is ca. 0.25 eV broad and is

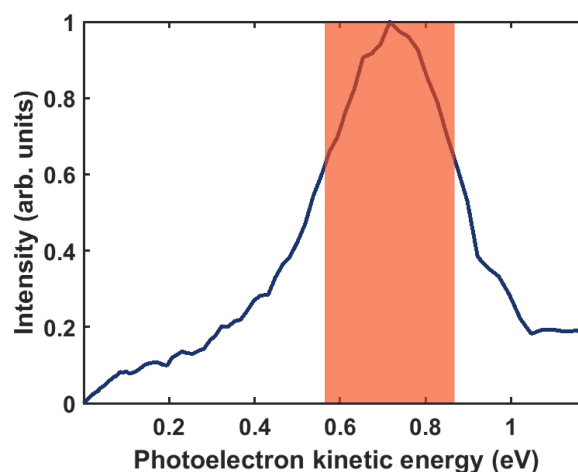


**Figure 2.** The photoelectron spectrum measured from methyl *p*-tolyl sulfoxide by ionisation of one photon of 133 nm light. The ionisation energy of methyl *p*-tolyl sulfoxide is 8.70 eV, which gives reasonable agreement with our measurement. The integration range for the evaluation of the photoelectron circular dichroism is highlighted in orange, and covers photoelectrons with kinetic energies between 0.58 and 0.85 eV.

centred at 0.7 eV. The width of the photoelectron spectrum is likely due to the fact that it spans a long vibrational progression originating from low-frequency modes. The integration region for the evaluation of the  $b_1$  parameter is indicated by the orange-shaded area, extending from 0.58 eV to 0.85 eV.

The PECD images of MTSO, and the fits of the angular distributions, are shown in Figure 3. The PECD image of *R*-(+)-MTSO is shown in panel a), and the PECD image of *S*-(-)-MTSO is shown in panel b). As one can see, the images are very similar in the magnitude of the signal, but mirror images of one another. This is exactly what one would expect. Panel c) shows the fitting of the photoelectron angular distribution of *R*-(+)-MTSO, and gives a  $2b_1$  value of  $0.24 \pm 0.03$ , and the corresponding fit of the *S*-(-)-MTSO (shown in panel d)) gives a  $2b_1$  value of  $-0.25 \pm 0.02$ . Aside from the fact that this value is remarkably high compared to previously studied molecules, there is extremely good agreement between the PECD from the two enantiomers.

We compared our experimentally determined PECD to calculated values obtained using a formalism introduced by Powis.<sup>[12]</sup> Using a geometry optimised at the RHF/cc-pVDZ level of theory, the photoionisation matrix elements were calculated using the ePolyScat program package to solve an electron-molecule scattering problem via the Schwinger variational principle.<sup>[44,45]</sup> Photoelectron angular distributions were obtained using a newly developed routine in the length gauge, yielding photoelectron kinetic energy (PKE)-dependent  $b_1$  values, which can be directly compared to the experiment. The photoelectron spectrum of MTSO was calculated using the outer-valence Green's function approach with the renormalised partial third-order approximation P3+ and the 6-311G\*\* basis set in Gaussian 09.<sup>[46]</sup> It was additionally compared with equation-of-motion coupled-cluster calculations (EOM-IP-CCSD/cc-pVTZ) performed in Orca 4.2.<sup>[47]</sup> These two methods showed

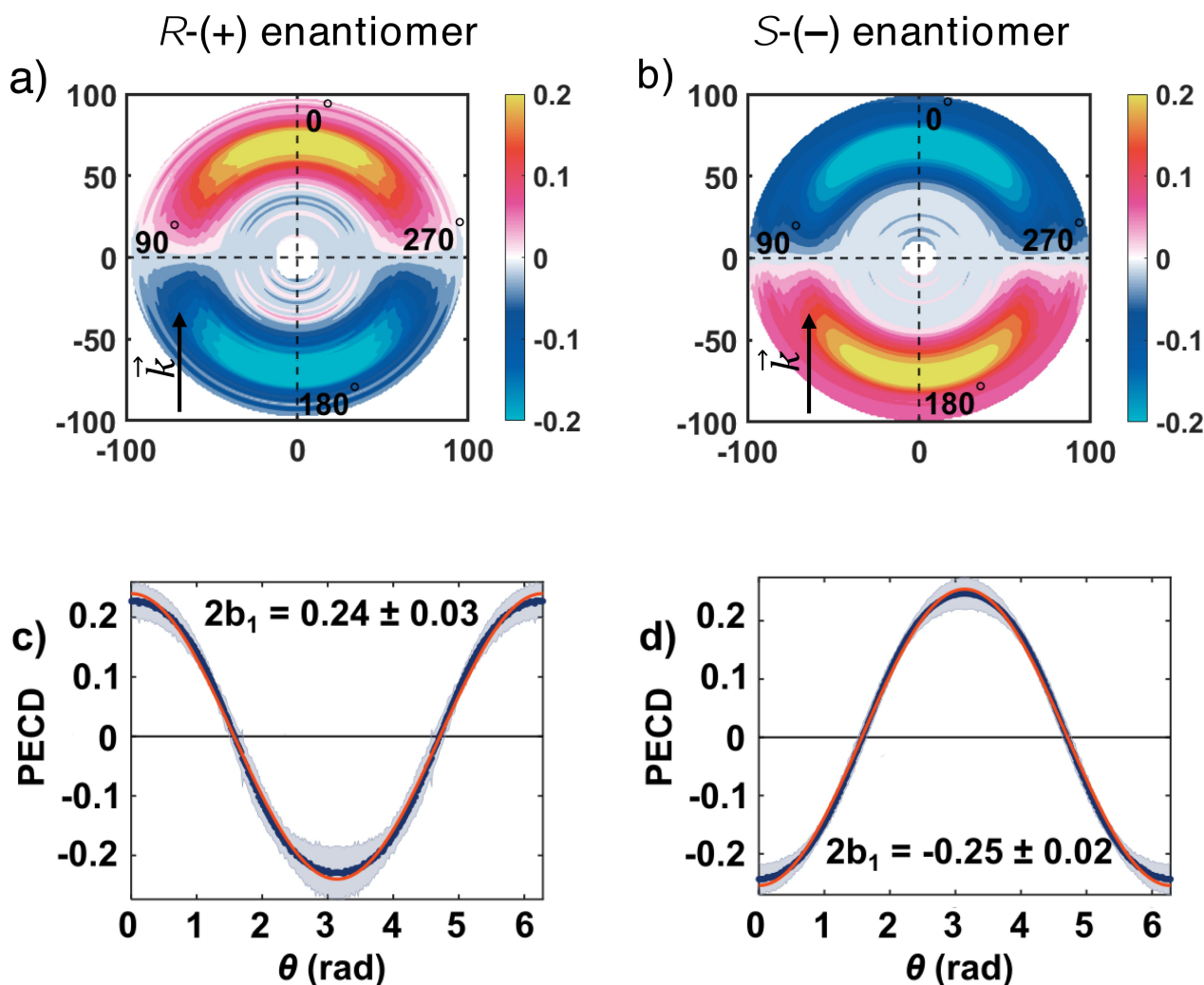


**Figure 3.** The antisymmetrised photoelectron circular dichroism images of *R*-(+)-methyl *p*-tolyl sulfoxide and *S*-(-)-methyl *p*-tolyl sulfoxide are shown in panel a) and b), respectively. The extracted angle-dependent  $2b_1$  parameters are displayed in panels c) and d) (blue, error bars in grey). The fitted cosines (red) according to eq. (2) show near perfect antisymmetry between the two images, returning  $2b_1 = 0.24 \pm 0.03$  for *R*-(+)-MTSO and  $2b_1 = -0.25 \pm 0.02$  for *S*-(-)-MTSO.

good agreement (as is seen in Figure 4) among themselves and with literature photoelectron spectra.<sup>[43]</sup> Specifically, the first band of the photoelectron spectrum (with a vertical ionisation potential of 8.7 eV)<sup>[43]</sup> is well separated from the next three bands with vertical ionisation energies of 9.5–10.0 eV.<sup>[43]</sup> The calculated ionisation energies of these lowest four electronic states of the cation are in excellent agreement with the measurements, up to an overall shift of 0.2–0.5 eV. Comparing the single broad peak in our photoelectron spectrum (Figure 2) with these results, we can therefore clearly conclude that our measurements exclusively access the electronic ground state of the MTSO cation. Through comparison of the RHF/cc-pVDZ geometry with the DFT geometry shown in Figure 1, and with high-resolution microwave spectroscopic measurements, we can exclude the presence of other conformers resulting from methyl rotations or rotations around the CCS=O dihedral angle.<sup>[48]</sup> Furthermore, a frequency analysis of our optimised structures reveals no imaginary frequencies, additionally con-

firming that they represent minima of the potential-energy surface.

Interestingly, the MTSO cation displays strong configuration interaction (CI), accompanied with a reordering of the molecular orbitals upon ionisation. This is visible from the sequence of the canonical Hartree–Fock (HF) orbitals describing the leading one-hole configuration of the molecular cation, displayed on top of Figure 4. Whereas the electronic ground state of the cation is dominated by a HOMO-hole configuration, the first excited state is dominated by a HOMO–2-hole configuration. Moreover, the two lowest-lying electronic states of the cation are configurationally mixed with the electronic ground-state wavefunction being described as possessing 58.4% of (HOMO)<sup>-1</sup> character and 36.5% of (HOMO–2)<sup>-1</sup> character. These values are obtained from the EOM-IP-CCSD/cc-pVTZ calculation.

The interesting question now is whether this strong CI has an impact on the PECD. Figure 5 shows the comparison between the calculated  $2b_1$  parameters for HOMO (panel a),

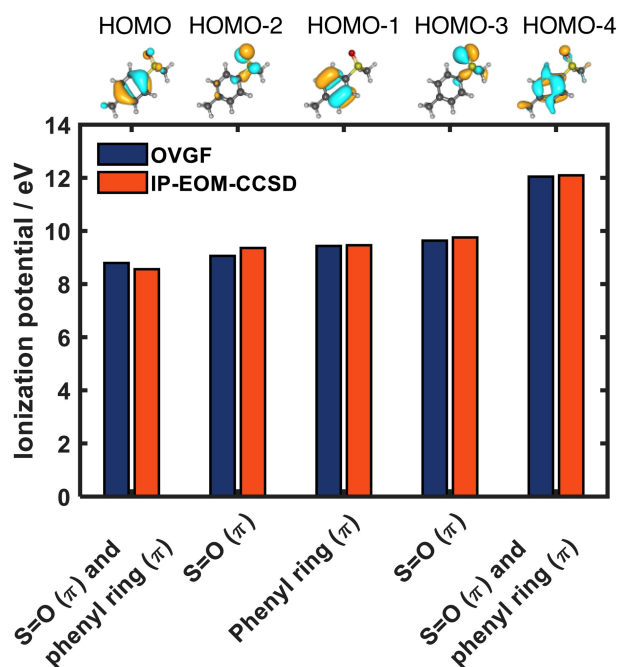


**Figure 4.** Calculated ionisation potentials of the first five cationic states of MTSO. The orange bars show the ionisation potentials evaluated at the IP-EOM-CCSD/cc-pVTZ level of theory, and the blue bars at the OVGf/6-311G\*\* level of theory (for more details, see the main text). The labels and orbital diagrams describe the dominant single-hole contributions to each cationic state.

HOMO–2 (b), the CI-weighted average of the two values (c) and our experimental measurements. In each case, the blue lines represent the *R*(+)-enantiomer, and the red lines represent the *S*(–)-enantiomer. The measured values for each enantiomer are shown by dashed lines, while the calculated values are shown by the solid lines, with crosses marking the photoelectron kinetic energies that the  $2b_1$  parameter is evaluated at. The calculated results for each enantiomer are identical in magnitude, but opposite in sign, with a general trend that increasing

the photoelectron kinetic energy decreases the magnitude of the asymmetry parameter. This can be rationalised by the fact that faster photoelectrons are scattered less strongly by the chiral potential. The mean of the three data points within the blue-shaded area is evaluated for each enantiomer.

Clearly, neither the calculated PECD values of HOMO (panel a), nor of HOMO–2 (panel b) agree with the experimental results, whereas the CI-weighted average of the PECD values (panel c) is in quantitative agreement with the experimental results.

This excellent match between the calculated and measured PECD value has only been achieved by accounting for configuration interaction in the cationic ground state. However, some words of caution are appropriate, since there are multiple factors which contribute to the magnitude of the  $b_1$  parameters. For example, the ePolyScat calculation describes the orbitals only in the Hartree–Fock picture, i.e. it neglects CI between the bound states of the cation, but also between the scattering (continuum) states. Our CI-weighting of the PECD values roughly accounts for CI between the electronic states of the cation, but it neglects CI between the scattering states, also known as channel couplings.<sup>[49]</sup> More elaborate methods, such as the multi-channel version of the basis-set complex-Kohn variational method can be used in the future to study these additional effects,<sup>[50,51]</sup> although these methods have – to our knowledge – not yet been applied to chiral molecules. Nevertheless, it is very encouraging to see such an excellent agreement between the theoretical and experimental values, which supports the robustness of this approach.

The sulfoxide functional group is one that occurs in a large number of chiral medicinal drugs. The ionised orbitals both show a remarkably strong PECD, and the strength of the PECD has been shown to be related to the strength of the scattering that the effective molecular potential exerts on the outgoing electron. These results are therefore very promising for the application of this methodology to enantiomeric characterisation of sulfoxide containing drugs, particularly as many pharmaceutical compounds contain large, electron rich, con-

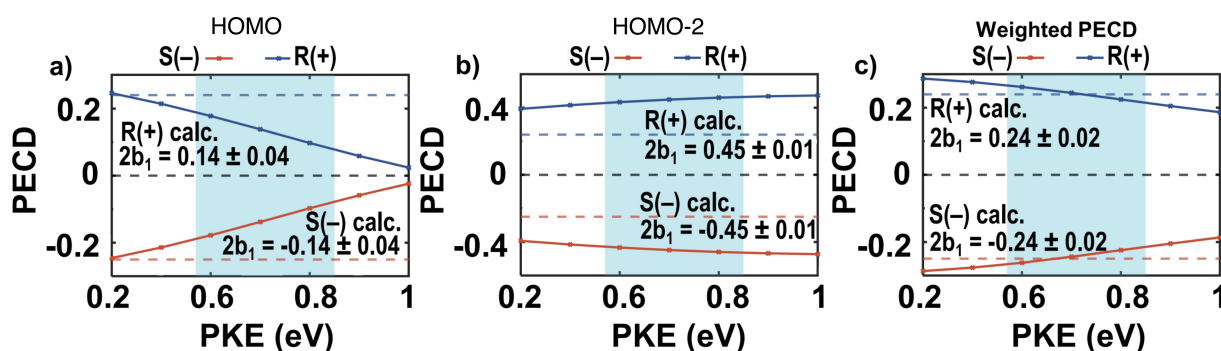


**Figure 5.** Photon-energy-dependent *ab initio* scattering calculations of the expected PECD parameters by single-photon ionisation of methyl *p*-tolyl sulfoxide. The blue-shaded area shows the integration region for the evaluation of the experimental  $2b_1$  values which are then shown by the red and blue dotted lines. Red refers to the *S*-enantiomer, and blue refers to the *R*-enantiomer. a) Shows the PECD contribution following ionisation from the HOMO, b) shows the PECD following ionisation from HOMO–2, and c) shows the total PECD following ionisation to the cationic ground state, obtained by weighting the single-orbital PECDs with the CI weights (0.584 of HOMO and 0.365 of HOMO–2 character). The calculated  $2b_1$  values within the shaded areas are averaged, giving the calculated values displayed in the plot of  $R = 0.24 \pm 0.02$  and  $S = -0.24 \pm 0.02$ , which is in quantitative agreement with the experiment.

jugated moieties, which could be expected to scatter reasonably strongly.

## Conclusions

In summary, this work presents single-photon PECD measurements of enantiopure methyl *p*-tolyl sulfoxide, resulting from ionisation of the highest-occupied molecular orbital with circularly polarised laser light. The PECD was observed using a velocity-map-imaging spectrometer, and the light was produced via high-harmonic generation. Our work presents a methodology for laboratory-based molecular chirality experiments with a tabletop source of high-energy photons. The chiral asymmetry parameter,  $2b_{11}$ , is found to be  $0.24 \pm 0.03$  for *R*-MTSO, and  $-0.25 \pm 0.02$  for *S*-MTSO. More generally, these results establish the considerable potential of the demonstrated experimental and theoretical methods for accessing valence-shell PECDs. The demonstrated source indeed possesses the ideal photon energy to realize time-resolved PECD measurements of photochemical dynamics. On one hand, it is low enough to create slow photoelectrons that are known to display large PECDs and on the other, it is high enough to ionise most chiral molecules and radicals from their electronic ground state, enabling complete photochemical reaction pathways to be followed by time-resolved PECD, opening the research area of femtochirality.

## Acknowledgement

This work has received funding from ETH Zürich, the NCCR-MUST, a funding instrument of the Swiss National Science Foundation and the Deutsche Forschungsgemeinschaft (DFG) – Project No. 328961117 – SFB 1319 ELCH (Extreme light for sensing and driving molecular chirality). Open Access funding provided by Eidgenössische Technische Hochschule Zürich.

## Conflict of Interest

The authors declare no conflict of interest.

## Data Availability Statement

The data that support the findings of this study are available from the corresponding author upon reasonable request.

**Keywords:** chirality · high harmonic generation · photoelectron circular dichroism · methyl *para*-tolyl sulfoxide · velocity map imaging

[1] S. W. Smith, *Toxicol. Sci.* **2009**, *110*, 4–30.

[2] L. D. Barron, *Molecular Light Scattering and Optical Activity*, Cambridge University Press, 2nd ed., **2004**.

- [3] U. Meierhenrich, *Amino Acids and the Asymmetry of Life*, Springer-Verlag Berlin Heidelberg, 1st ed., **2008**.
- [4] E. Hirota, *Proc. Jpn. Acad. Ser. B* **2012**, *88*, 120–128.
- [5] D. Patterson, J. M. Doyle, *Phys. Rev. Lett.* **2013**, *111*, 023008.
- [6] D. Patterson, M. Schnell, J. M. Doyle, *Nature* **2013**, *497*, 475–477.
- [7] M. Pitzer, M. Kunitski, A. S. Johnson, T. Jahnke, H. Sann, F. Sturm, L. P. H. Schmidt, H. Schmidt-Böcking, R. Dörner, J. Stohner, J. Kiedrowski, M. Reggelin, S. Marquardt, A. Schießler, R. Berger, M. S. Schöffler, *Science* **2013**, *341*, 1096–1100.
- [8] D. Baykusheva, H. J. Wörner, *Phys. Rev. X* **2018**, *8*, 031060.
- [9] D. Baykusheva, D. Zindel, V. Svoboda, E. Bommeli, M. Ochsner, A. Tehlar, H. J. Wörner, *Proc. Natl. Acad. Sci. USA* **2019**, *116*, 23923–23929.
- [10] B. Ritchie, *Phys. Rev. A* **1976**, *13*, 1411–1415.
- [11] N. Böwering, T. Lischke, B. Schmidtke, N. Müller, T. Khalil, U. Heinzmann, *Phys. Rev. Lett.* **2001**, *86*, 1187–1190.
- [12] I. Powis, *J. Chem. Phys.* **2000**, *112*, 301–310.
- [13] C. Lux, M. Wollenhaupt, T. Bolze, Q. Liang, J. Köhler, C. Sarpe, T. Baumert, *Angew. Chem. Int. Ed.* **2012**, *51*, 5001–5005; *Angew. Chem.* **2012**, *124*, 5086–5090.
- [14] M. H. M. Janssen, I. Powis, *Phys. Chem. Chem. Phys.* **2014**, *16*, 856–871.
- [15] A. F. Ordonez, O. Smirnova, *Phys. Rev. A* **2019**, *99*, 043416.
- [16] L. Nahon, G. A. Garcia, I. Powis, *J. Electron Spectrosc. Relat. Phenom.* **2015**, *202*, 322–334.
- [17] A. Comby, S. Beaulieu, M. Boggio-Pasqua, D. Descamps, F. Légaré, L. Nahon, S. Petit, B. Pons, B. Fabre, Y. Mairesse, V. Blanchet, *J. Phys. Chem. Lett.* **2016**, *7*, 4514–4519.
- [18] A. Kastner, C. Lux, T. Ring, S. Züllighoven, C. Sarpe, A. Senftleben, T. Baumert, *ChemPhysChem* **2016**, *17*, 1119–1122.
- [19] A. Kastner, G. Koumariou, P. Glodic, P. C. Samartzis, N. Ladda, S. T. Raney, T. Ring, S. Vasudevan, C. Witte, H. Braun, H.-G. Lee, A. Senftleben, R. Berger, G. B. Park, T. Schäfer, T. Baumert, *Phys. Chem. Chem. Phys.* **2020**, *22*, 7404–7411.
- [20] C. J. Harding, E. Mikajlo, I. Powis, S. Barth, S. Joshi, V. Ulrich, U. Hergenhan, *J. Chem. Phys.* **2005**, *123*, 234310.
- [21] M. Tia, M. Pitzer, G. Kastirke, J. Gatzke, H.-K. Kim, F. Trinter, J. Rist, A. Hartung, D. Trabert, J. Siebert, K. Henrichs, J. Becht, S. Zeller, H. Gassert, F. Wiegandt, R. Wallauer, A. Kuhlins, C. Schober, T. Bauer, M. Wechselberger, P. Burzynski, J. Neff, M. Weller, D. Metz, M. Kircher, M. Waitz, J. B. Williams, L. P. H. Schmidt, A. D. Müller, A. Knie, A. Hans, L. Ben Ltaief, A. Ehresmann, R. Berger, H. Fukuzawa, K. Ueda, H. Schmidt-Böcking, R. Dörner, T. Jahnke, P. V. Demekhin, M. Schöffler, *J. Phys. Chem. Lett.* **2017**, *8*, 2780–2786.
- [22] K. Fehre, N. M. Novikovskiy, S. Grundmann, G. Kastirke, S. Eckart, F. Trinter, J. Rist, A. Hartung, D. Trabert, C. Janke, G. Nalin, M. Pitzer, S. Zeller, F. Wiegandt, M. Weller, M. Kircher, M. Hofmann, L. P. H. Schmidt, A. Knie, A. Hans, L. B. Ltaief, A. Ehresmann, R. Berger, H. Fukuzawa, K. Ueda, H. Schmidt-Böcking, J. B. Williams, T. Jahnke, R. Dörner, M. S. Schöffler, P. V. Demekhin, *Phys. Rev. Lett.* **2021**, *127*, 103201.
- [23] L. Nahon, G. A. Garcia, C. J. Harding, E. Mikajlo, I. Powis, *J. Chem. Phys.* **2006**, *125*, 114309.
- [24] M. Stener, D. Di Tommaso, G. Fronzoni, P. Declava, I. Powis, *J. Chem. Phys.* **2006**, *124*, 024326.
- [25] A. Ferré, C. Handschin, M. Dumergue, F. Burgy, A. Comby, D. Descamps, B. Fabre, G. Garcia, R. Géneaux, L. Merceron et al, *Nat. Photonics* **2015**, *9*, 93–98.
- [26] V. Svoboda, M. D. J. Waters, D. Zindel, H. J. Wörner, *Opt. Express* **2022**, *30*, 14358–14367.
- [27] V. Svoboda, N. B. Ram, R. Rajeev, H. J. Wörner, *J. Chem. Phys.* **2017**, *146*, 084301.
- [28] A. von Conta, A. Tehlar, A. Schletter, Y. Arasaki, K. Takatsuka, H. J. Wörner, *Nat. Commun.* **2018**, *9*, 3162.
- [29] V. Svoboda, C. Wang, M. D. J. Waters, H. J. Wörner, *J. Chem. Phys.* **2019**, *151*, 104306.
- [30] T. Horio, R. Spesyvtsev, K. Nagashima, R. A. Ingle, Y.-i. Suzuki, T. Suzuki, *J. Chem. Phys.* **2016**, *145*, 044306.
- [31] T. Horio, R. Spesyvtsev, Y. Furumido, T. Suzuki, *J. Chem. Phys.* **2017**, *147*, 013932.
- [32] N. Kotsina, D. Townsend, *Phys. Chem. Chem. Phys.* **2021**, *23*, 10736–10755.
- [33] S. Beaulieu, A. Ferré, R. Géneaux, R. Canonge, D. Descamps, B. Fabre, N. Fedorov, F. Légaré, S. Petit, T. Ruchon, V. Blanchet, Y. Mairesse, B. Pons, *New J. Phys.* **2016**, *18*, 102002.
- [34] M. Wollenhaupt, *New J. Phys.* **2016**, *18*, 121001.

- [35] B. Darquié, N. Saleh, S. K. Tokunaga, M. Srebro-Hooper, A. Ponzi, J. Autschbach, P. Decleva, G. A. Garcia, J. Crassous, L. Nahon, *Phys. Chem. Chem. Phys.* **2021**, *23*, 24140–24153.
- [36] G. S. Sankaran, S. Arumugan, S. Balasubramaniam, *MOJ Bioorg. Org. Chem.* **2018**, *2*, 93–101.
- [37] J. Han, V. A. Soloshonok, K. D. Klika, J. Drabowicz, A. Wzorek, *Chem. Soc. Rev.* **2018**, *47*, 1307–1350.
- [38] P. Diter, S. Taudien, O. Samuel, H. B. Kagan, *J. Org. Chem.* **1994**, *59*, 370–373.
- [39] A. Wzorek, K. D. Klika, J. Drabowicz, A. Sato, J. L. Aceña, V. A. Soloshonok, *Org. Biomol. Chem.* **2014**, *12*, 4738–4746.
- [40] S. Gibson, D. D. Hickstein, R. Yurchak, M. Ryazanov, D. Das, G. Shih, PyAbel/PyAbel: v. 0.8.4, **2021**, <https://doi.org/10.5281/zenodo.4690660>.
- [41] I. Powis in *Photoelectron Circular Dichroism in Chiral Molecules*, John Wiley & Sons, Ltd, **2008**, Chapter 5, pp. 267–329.
- [42] L. Nahon, L. Nag, G. A. Garcia, I. Myrgorodska, U. Meierhenrich, S. Beaulieu, V. Wanie, V. Blanchet, R. Généaux, I. Powis, *Phys. Chem. Chem. Phys.* **2016**, *18*, 12696–12706.
- [43] M. Mohraz, W. Jian-qi, E. Heilbronner, A. Solladiéa-Cavallo, F. Matloubi-Moghadam, *Helv. Chim. Acta* **1981**, *64*, 97–112.
- [44] F. A. Gianturco, R. R. Lucchese, N. Sanna, *J. Chem. Phys.* **1994**, *100*, 6464–6471.
- [45] A. P. P. Natalense, R. R. Lucchese, *J. Chem. Phys.* **1999**, *111*, 5344–5348.
- [46] J. V. Ortiz, *Int. J. Quantum Chem.* **2005**, *105*, 803–808.
- [47] F. Neese, *WIREs Comput. Mol. Sci.* **2018**, *8*, e1327.
- [48] W. Sun, I. Kleiner, A. Senftleben, M. Schnell, *J. Chem. Phys.* **2022**, *156*, 154304.
- [49] M. Mohan, K. L. Baluja, V. Prasad, A. Hibbert, *J. Phys. B: At. Mol. Opt. Phys.* **1991**, *24*, 3889–3894.
- [50] T. N. Rescigno, B. H. Lengsfeld III, C. W. McCurdy in *Modern Electronic Structure Theory*, Vol. 1 (Ed.: D. R. Yarkony), World Scientific, Singapore, **1995**, pp. 501–588.
- [51] T. N. Rescigno, C. W. McCurdy, A. E. Orel, B. H. Lengsfeld III in *Computational Methods for Electron-Molecule Collisions*, Springer, **1995**, pp. 1–44.
- [52] M. J. Frisch, G. W. Trucks, H. B. Schlegel, G. E. Scuseria, M. A. Robb, J. R. Cheeseman, G. Scalmani, V. Barone, B. Mennucci, G. A. Petersson, H. Nakatsuji, M. Caricato, X. Li, H. P. Hratchian, A. F. Izmaylov, J. Bloino, G. Zheng, J. L. Sonnenberg, M. Hada, M. Ehara, K. Toyota, R. Fukuda, J. Hasegawa, M. Ishida, T. Nakajima, Y. Honda, O. Kitao, H. Nakai, T. Vreven, J. A. Montgomery, Jr., J. E. Peralta, F. Ogliaro, M. Bearpark, J. J. Heyd, E. Brothers, K. N. Kudin, V. N. Staroverov, R. Kobayashi, J. Normand, K. Raghavachari, A. Rendell, J. C. Burant, S. S. Iyengar, J. Tomasi, M. Cossi, N. Rega, J. M. Millam, M. Klene, J. E. Knox, J. B. Cross, V. Bakken, C. Adamo, J. Jaramillo, R. Gomperts, R. E. Stratmann, O. Yazyev, A. J. Austin, R. Cammi, C. Pomelli, J. W. Ochterski, R. L. Martin, K. Morokuma, V. G. Zakrzewski, G. A. Voth, P. Salvador, J. J. Dannenberg, S. Dapprich, A. D. Daniels, Ö. Farkas, J. B. Foresman, J. V. Ortiz, J. Cioslowski, D. J. Fox, *Gaussian 09 Revision E.01*, Gaussian Inc. Wallingford CT **2009**.
- [53] T. Moitra, A. Ponzi, H. Koch, S. Coriani, P. Decleva, *J. Phys. Chem. Lett.* **2020**, *11*, 5330–5337.
- [54] T. Moitra, S. Coriani, P. Decleva, *J. Chem. Theory Comput.* **2021**, *17*, 5064–5079.

---

Manuscript received: August 2, 2022  
Revised manuscript received: August 12, 2022  
Accepted manuscript online: August 15, 2022  
Version of record online: September 19, 2022